The Slantlet Transform

Ivan W. Selesnick, *Member, IEEE*

***Abstract*— The discrete wavelet transform (DWT) is usually carried out by filterbank iteration; however, for a fixed number of zero moments, this does not yield a discrete-time basis that is optimal with respect to time localization. This paper discusses the implementation and properties of an orthogonal DWT, with two zero moments and with improved time localization. The basis is not based on filterbank iteration; instead, different filters are used for each scale. For coarse scales, the support of the discrete-time basis functions approaches two thirds that of the corresponding functions obtained by filterbank iteration. This basis, which is a special case of a class of bases described by Alpert, retains the octave-band characteristic and is piecewise linear (but discontinuous). Closed-form expressions for the filters are given, an efficient implementation of the transform is described, and improvement in a denoising example is shown. This basis, being piecewise linear, is reminiscent of the slant transform, to which it is compared.**

I. Introduction

Discrete wavelet transforms (DWT's) are useful in a variety of applications (such as estimation, compression, and fast algorithms), partly because they can provide relatively efficient representations of piecewise smooth signals [9], [30]. The degree to which a wavelet basis can successfully yield sparse representations of such signals depends on the time-localization and smoothness properties of the basis functions. For example, signal smoothing by the nonlinear thresholding of DWT coefficients [14] preserves edges reasonably well—in part, because the support of each basis function is short with respect to its bandwidth. (Thus, we have the "constant-Q" behavior, or octave-band characteristic, of the associated filterbank.) However, a fundamental tradeoff exists between time localization and smoothness characteristics, and it is desirable to obtain a good tradeoff between these two competing criteria in designing wavelet bases. As is usual for DWT's, in this paper, the lengths of the discrete-time basis functions and their moments are the vehicles by which time localization and smoothness properties are achieved.

Although the usual filterbank iteration provides a simple way to generate an orthogonal discrete-time basis having an octave-band characteristic, for a fixed number of zero moments, it does not yield a discrete-time basis that is optimal with respect to time localization. This paper examines a special case of a class of bases originally described by Alpert in [4]–[6] in a multiwavelet context, the construction of which relies on Gram–Schmidt orthogonalization. We describe the basis from a filterbank viewpoint, give explicit solutions for the filter coefficients, and describe an efficient algorithm for the transform.

The DWT described in this paper is based on a filterbank structure where (as in [2] and [3]) different filters are used for each scale. Nevertheless, a very simple efficient algorithm based on recursion is available. For the DWT filterbank described here, the support of the discrete-time basis functions is reduced (by a factor approaching one third for coarse scales) while retaining the basic characteristics of the two-band iterated filterbank tree. This basis retains the octave-band characteristic and leads cleanly to a DWT for finite length signals (boundary issues do not arise, provided the data length is a power of 2). The filters are piecewise linear but are discontinuous—for coarse scales, they converge to piecewise linear, discontinuous functions.

The basis, being piecewise linear, is reminiscent of the slant transform to which it is compared. However, the basis functions of the slant transform, like the Hadamard transform for example, are nonzero over all of the domain, whereas the basis functions described in this paper become progressively more narrow, giving a multiresolution decomposition. Hence, we have the name slantlet for the transform described here. The slantlet basis appears especially well suited for treating piecewise linear signals, as is supported by the denoising example below.

II. Slantlet Filterbank

It is useful to consider first the usual iterated DWT filterbank and an equivalent[1] form, which is shown in Fig. 1. The "slantlet" filterbank described here is based on the second structure, but it will be occupied by different filters that are not products. With the extra degrees of freedom obtained by giving up the product form, it is possible to design filters of shorter length while satisfying orthogonality and zero moment conditions, as will be shown.

For the two-channel case, the shortest filters for which the filterbank is orthogonal and has K zero moments are the well-known filters described by Daubechies [13]. For $K = 2$ zero moments, those filters $H(z)$ and $F(z)$ are of length 4. For this system, which is designated D_2, the iterated filters in Fig. 1

[1] Note that interleaving the third and fourth channels of the second structure gives the third channel of the first structure. Because that difference is unimportant for our purpose, in this paper, the two structures will be considered equivalent

Manuscript received February 17, 1998; revised November 9, 1998. This work was supported by the Alexander von Humboldt Foundation. The associate editor coordinating the review of this paper and approving it for publication was Dr. Akram Aldroubi.

The author is with Electrical Engineering, Polytechnic University, Brooklyn, NY 11201 USA (e-mail: selesi@taco.poly.edu).

Publisher Item Identifier S 1053-587X(99)03233-X.

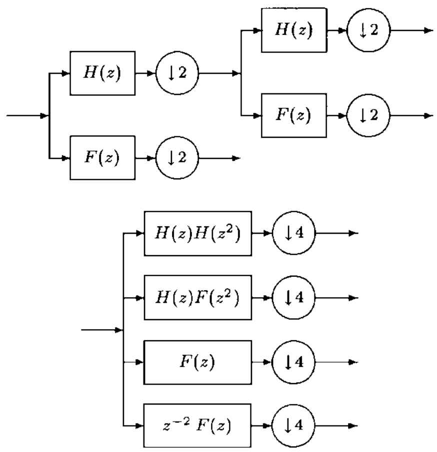

Fig. 1. Two-scale filterbank and an equivalent structure.

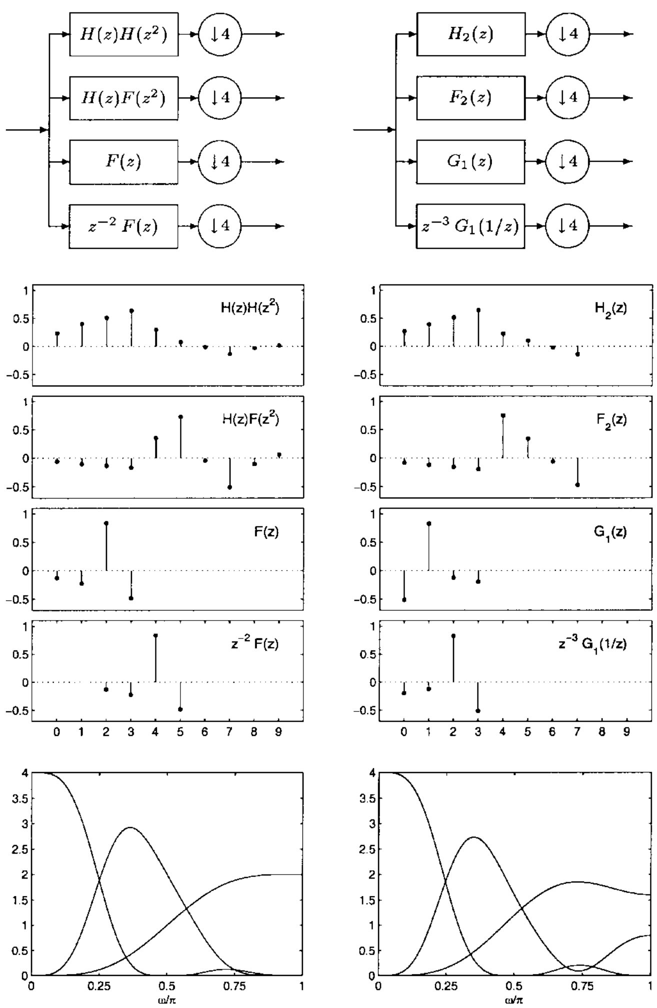

Fig. 2. Comparison of two-scale iterated D_2 filterbank (left-hand side) and two-scale slantlet filterbank (right-hand side).

are of length 10 and 4. Without the constraint that the filters are products, an orthogonal filterbank with $K = 2$ zero moments can be obtained where the filter lengths are 8 and 4, as shown in Fig. 2, side by side with the iterated D_2 system. That is a reduction by two samples, which is a difference that grows with the number of stages, as will be shown.

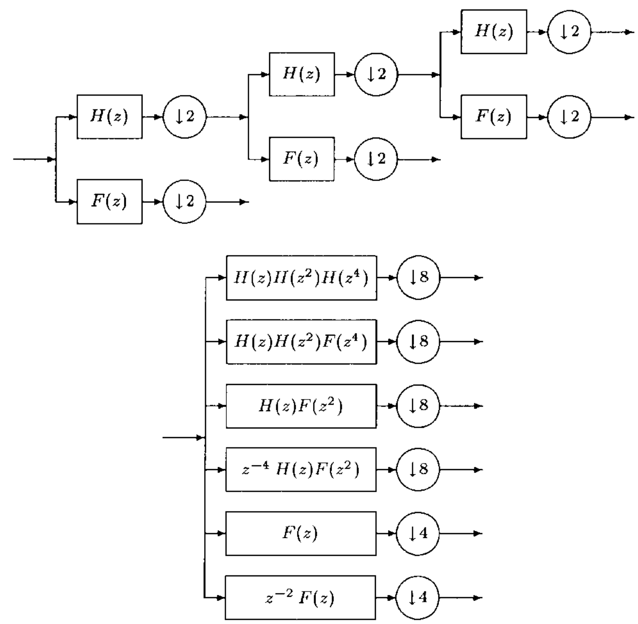

Fig. 3. Three-scale filterbank and an equivalent structure.

The filters shown on the right-hand side of Fig. 2 are

$$\begin{aligned} G_1(z) = {} & \left(-\frac{\sqrt{10}}{20} - \frac{\sqrt{2}}{4}\right) + \left(\frac{3\sqrt{10}}{20} + \frac{\sqrt{2}}{4}\right) z^{-1} \\ & + \left(-\frac{3\sqrt{10}}{20} + \frac{\sqrt{2}}{4}\right) z^{-2} + \left(\frac{\sqrt{10}}{20} - \frac{\sqrt{2}}{4}\right) z^{-3} \end{aligned}$$

$$\begin{aligned} F_2(z) = {} & \left(\frac{7\sqrt{5}}{80} - \frac{3\sqrt{55}}{80}\right) + \left(-\frac{\sqrt{5}}{80} - \frac{\sqrt{55}}{80}\right) z^{-1} \\ & + \left(-\frac{9\sqrt{5}}{80} + \frac{\sqrt{55}}{80}\right) z^{-2} + \left(-\frac{17\sqrt{5}}{80} + \frac{3\sqrt{55}}{80}\right) z^{-3} \\ & + \left(\frac{17\sqrt{5}}{80} + \frac{3\sqrt{55}}{80}\right) z^{-4} + \left(\frac{9\sqrt{5}}{80} + \frac{\sqrt{55}}{80}\right) z^{-5} \\ & + \left(\frac{\sqrt{5}}{80} - \frac{\sqrt{55}}{80}\right) z^{-6} + \left(-\frac{7\sqrt{5}}{80} - \frac{3\sqrt{55}}{80}\right) z^{-7} \end{aligned}$$

$$\begin{aligned} H_2(z) = {} & \left(\frac{1}{16} + \frac{\sqrt{11}}{16}\right) + \left(\frac{3}{16} + \frac{\sqrt{11}}{16}\right) z^{-1} \\ & + \left(\frac{5}{16} + \frac{\sqrt{11}}{16}\right) z^{-2} + \left(\frac{7}{16} + \frac{\sqrt{11}}{16}\right) z^{-3} \\ & + \left(\frac{7}{16} - \frac{\sqrt{11}}{16}\right) z^{-4} + \left(\frac{5}{16} - \frac{\sqrt{11}}{16}\right) z^{-5} \\ & + \left(\frac{3}{16} - \frac{\sqrt{11}}{16}\right) z^{-6} + \left(\frac{1}{16} - \frac{\sqrt{11}}{16}\right) z^{-7}. \end{aligned}$$

Fig. 3 illustrates a three-scale filterbank tree for the DWT and, again, an equivalent structure. The three-scale iterated D_2 filterbank tree analyzes signals at three scales with filters of length 4, 10, and 22, as illustrated on the left-hand side of Fig. 4. On the other hand, the filterbank shown on the right-hand side of Fig. 4 analyzes a signal at three scales with

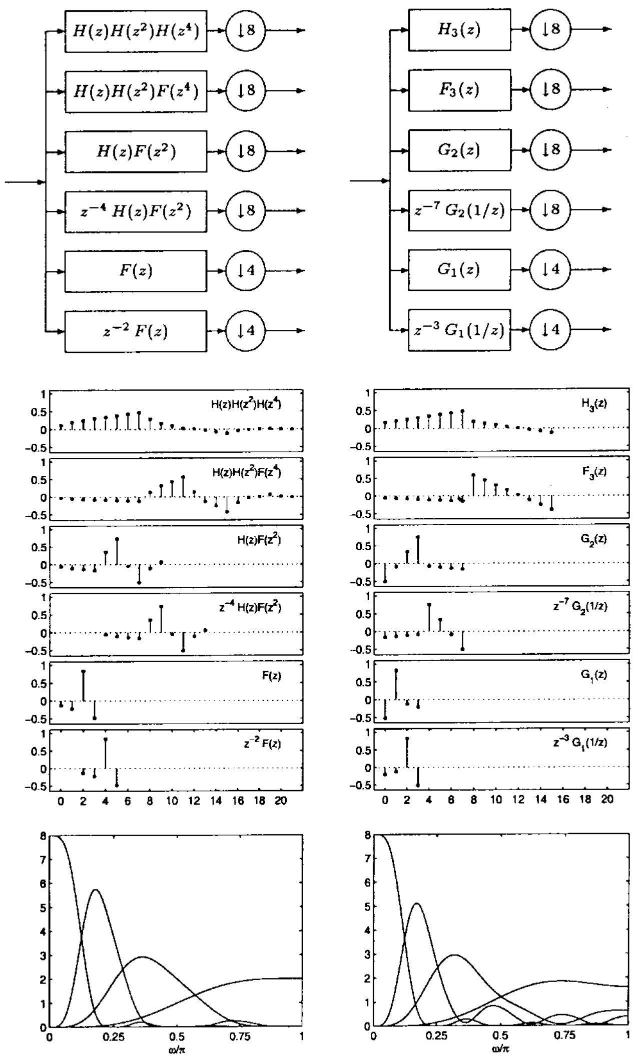

Fig. 4. Comparison of three-scale iterated D_2 filterbank (left-hand side) and three-scale slantlet filterbank (right-hand side).

filters of length 4, 8, and 16. This reduction in length, while maintaining desirable orthogonality and moment properties, is possible because these filters are not constrained by the product form arising in the case of iterated filterbanks.

We make several comments regarding Figs. 2 and 4.

1) Each filterbank (equivalently, discrete-time basis) is orthogonal. The filters in the synthesis filterbank are obtained by time reversal of the analysis filters.
2) Each filterbank has two zero moments. The filters (except for the lowpass ones) annihilate discrete-time polynomials of degree less than 2.
3) Each filterbank has an octave-band characteristic.
4) The scale-dilation factor is 2 for each filterbank. Between scales, the filters dilate by roughly a factor of 2. (In the slantlet filterbanks, they dilate by exactly a factor of 2.)
5) Each filterbank provides a multiresolution decomposition. By discarding the highpass channels and passing only the lowpass channel outputs through the synthesis filterbank, a lower resolution version of the original signal is obtained.
6) The slantlet filterbank is less frequency selective than the traditional DWT filterbank due to the shorter length of the filters. The time localization is improved with a degradation of frequency selectivity.
7) The slantlet filters are piecewise linear.

It must be admitted that although both types of filterbanks posses the same number of zero moments, the smoothness properties of the filters are somewhat different. In Figs. 2 and 4, the slantlet filters have greater "jumps" than do the iterated D_2 filters—that is, they have a greater maximum difference between adjacent sample values. The Haar basis, with its discontinuities, is suitable for analyzing piecewise constant functions. Likewise, the slantlet filterbank appears appropriate for the analysis of piecewise linear functions with discontinuities, as illustrated in the denoising example below. The ability to model discontinuities is also relevant for other applications, like edge detection and change point analysis, in which the detection of abrupt changes in an otherwise relatively smooth but unknown function is considered [24], [27].

We also wish to mention that symmetry of the filters is an important property in some applications, especially in image processing. While the filters described here are not symmetric, the filters $g_i(n)$ are paired with their time-reversed versions so that the effect of time reversing the input signal on the g_i channels is merely an interchange of adjacent the channels.

A. Notation

We will denote, by scale i, the scale with which $g_i(n)$, $f_i(n)$, and $h_i(n)$ analyze a signal. The length of the filters for scale i will be proportional to 2^i. That is approximately true for iterated filterbanks; however, it is exact for slantlet filterbanks. In general, the support of $g_i(n)$, $f_i(n)$, and $h_i(n)$ will be 2^{i+1}.

We should clarify the way in which the slantlet filterbanks in Figs. 2 and 4 are generalized to l scales. That is done as follows. The l-scale filterbank has $2l$ channels. The lowpass filter is to be called $h_l(n)$. The filter adjacent to the lowpass channel is to be called $f_l(n)$. Both $h_l(n)$ and $f_l(n)$ are to be followed by downsampling by 2^l. The remaining $2l-2$ channels are filtered by $g_i(n)$ and its shifted time-reverse for $i = 1, \ldots, l-1$. Each is to be followed by downsampling by 2^{i+1}. It follows that the filterbank is critically sampled.

Note that in the slantlet filterbank, each filter $g_i(n)$ appears together with its time reverse. While $h_i(n)$ does not appear with its time reverse, it always appears paired with the filter $f_i(n)$. In addition, note that the l-scale and $(l+1)$-scale filterbanks have in common the filters $g_i(n)$ for $i = 1, \ldots, l-1$ and their time-reversed versions.

B. Derivations

That the sought filters $g_i(n)$, $f_i(n)$, and $h_i(n)$ are piecewise linear is central to the following derivation. When coupled with the zero moments, it simplifies orthogonality conditions. First, suppose that $g_i(n)$, $f_i(n)$, and $h_i(n)$ are each linear over the interval $n \in \{0, \ldots, 2^i - 1\}$ and over the interval $n \in \{2^i, \ldots, 2^{i+1} - 1\}$, as in Figs. 2 and 4. Suppose, in addition, that $g_i(n)$ and $f_i(n)$ have two zero moments—that is, their inner products with linear polynomial sequences are zero [as filters, $g_i(n)$ and $f_i(n)$ annihilate "ramps"]. With $j > i$, over the support of $g_i(n)$, the functions $g_j(n)$, $f_j(n)$, and $h_j(n)$ are linear so that orthogonality between scales is immediate. The same is true for the appropriately shifted versions $g_i(n-2^i)$, $f_i(n-2^i)$, and their time-reversed versions.

Because the sought-after filter $g_i(n)$ is to be linear over the two above-mentioned intervals, it is described by four parameters and can be written as

$$g_i(n) = \begin{cases} a_{0,0} + a_{0,1} n, & \text{for } n = 0, \dots 2^i - 1 \\ a_{1,0} + a_{1,1}(n - 2^i), & \text{for } n = 2^i, \dots 2^{i+1} - 1. \end{cases}$$

Therefore, to obtain $g_i(n)$ such that the sought-after l-scale filterbank is orthogonal with two zero moments requires obtaining parameters $a_{0,0}$, $a_{0,1}$, $a_{1,0}$, and $a_{1,1}$ so that we have the following.

1) $g_i(n)$ is of unit norm.

$$\sum_{n=0}^{2^{i+1}-1} g_i^2(n) = 1.$$

2) $g_i(n)$ is orthogonal to its shifted time reverse.

$$\sum_{n=0}^{2^{i+1}-1} g_i(n) g_i(2^{i+1} - 1 - n) = 0.$$

3) $g_i(n)$ annihilates linear discrete time polynomials.

$$\sum_{n=0}^{2^{i+1}-1} g_i(n) = 0, \qquad \sum_{n=0}^{2^{i+1}-1} n g_i(n) = 0.$$

Each of the conditions can be written as an algebraic equation in terms of the four parameters $a_{0,0}$, $a_{0,1}$, $a_{1,0}$, and $a_{1,1}$ to obtain a multivariate polynomial system of equations. The conditions are nonlinear in the four parameters; however, with assistance from the computer algebra systems *Maple* [11] and *Singular* [16] (for the computation of Gröbner bases), we obtain the following expressions for $g_i(n)$:

$$g_i(n) = \begin{cases} a_{0,0} + a_{0,1} n, & \text{for } n = 0, \dots 2^i - 1 \\ a_{1,0} + a_{1,1}(n - 2^i), & \text{for } n = 2^i, \dots 2^{i+1} - 1 \end{cases}$$

where

$$\begin{aligned} m &= 2^i \\ s_1 &= 6\sqrt{m/((m^2-1)(4m^2-1))} \\ t_1 &= 2\sqrt{3/(m \cdot (m^2-1))} \\ s_0 &= -s_1 \cdot (m-1)/2 \\ t_0 &= ((m+1) \cdot s_1/3 - m t_1)(m-1)/(2m) \\ a_{0,0} &= (s_0 + t_0)/2 \\ a_{1,0} &= (s_0 - t_0)/2 \\ a_{0,1} &= (s_1 + t_1)/2 \\ a_{1,1} &= (s_1 - t_1)/2. \end{aligned}$$

Note that the parameters $a_{0,0}$, $a_{0,1}$, $a_{1,0}$, and $a_{1,1}$ depend on i.

The same approach works for $f_i(n)$ and $h_i(n)$. Using, again, a piecewise linear form, $h_i(n)$ and $f_i(n)$ can be written in terms of eight unknown parameters $b_{0,0}$, $b_{0,1}$, $b_{1,0}$, $b_{1,1}$, $c_{0,0}$, $c_{0,1}$, $c_{1,0}$, and $c_{1,1}$.

$$h_i(n) = \begin{cases} b_{0,0} + b_{0,1} n, & \text{for } n = 0, \dots 2^i - 1 \\ b_{1,0} + b_{1,1}(n - 2^i), & \text{for } n = 2^i, \dots 2^{i+1} - 1 \end{cases}$$

$$f_i(n) = \begin{cases} c_{0,0} + c_{0,1} n, & \text{for } n = 0, \dots 2^i - 1 \\ c_{1,0} + c_{1,1}(n - 2^i), & \text{for } n = 2^i, \dots 2^{i+1} - 1. \end{cases}$$

The orthogonality and moment conditions require the following.

1) $h_i(n)$ and $f_i(n)$ are of unit norm.

$$\sum_{n=0}^{2^{i+1}-1} h_i^2(n) = 1. \qquad \sum_{n=0}^{2^{i+1}-1} f_i^2(n) = 1.$$

2) $h_i(n)$ and $f_i(n)$ are orthogonal to their shifted versions.

$$\sum_{n=0}^{2^i-1} h_i(n) h_i(n+2^i) = 0$$

$$\sum_{n=0}^{2^i-1} f_i(n) f_i(n+2^i) = 0$$

$$\sum_{n=0}^{2^{i+1}-1} h_i(n) f_i(n) = 0$$

$$\sum_{n=0}^{2^i-1} h_i(n) f_i(n+2^i) = 0.$$

3) $f_i(n)$ annihilates linear discrete time polynomials.

$$\sum_{n=0}^{2^{i+1}-1} f_i(n) = 0, \qquad \sum_{n=0}^{2^{i+1}-1} n f_i(n) = 0.$$

By expressing the orthogonality and moment conditions as a multivariate polynomial system, we obtain the following solution for $h_i(n)$ and $f_i(n)$:

$$\begin{aligned} m &= 2^i \\ u &= 1/\sqrt{m} \\ v &= \sqrt{(2m^2+1)/3} \\ b_{0,0} &= u \cdot (v+1)/(2m) \\ b_{1,0} &= u - b_{0,0} \\ b_{0,1} &= u/m \\ b_{1,1} &= -b_{0,1} \\ q &= \sqrt{3/(m \cdot (m^2-1))}/m \\ c_{0,1} &= q \cdot (v - m) \\ c_{1,1} &= -q \cdot (v + m) \\ c_{1,0} &= c_{1,1} \cdot (v + 1 - 2m)/2 \\ c_{0,0} &= c_{0,1} \cdot (v+1)/2. \end{aligned}$$

In these expression for $g_i(n)$, $f_i(n)$, and $h_i(n)$, the signs of any of the square roots can be negated. Doing so merely negates or time reverses the sequences.

We note that $h_i(n)$ and $f_i(n)$ specialize to the Daubechies length-4 filters for $i = 1$, as expected.

C. Support Length

In Figs. 2 and 4, it was seen that the support of the slantlet filters is less than those of the filters obtained by filterbank iteration. It is interesting to note the difference for the general l-scale case. The iterated filterbank, with Daubechies length-4 filters, analyzes scale i with a filter of length $3 \cdot 2^i - 2$. On the other hand, the slantlet filterbank analyzes scale i with the filter $g_i(n)$ of length 2^{i+1}. That gives a reduction of $2^i - 2$ samples for scale i. The ratio tends to two thirds as i increases (for coarser scales). That reduction in the support of the analysis filters is precisely what was sought.

D. Multiresolution Spaces

To clarify the multiresolution spaces generated by the filterbanks described in this paper, it is convenient to define appropriate function spaces, as is usually done.

$$\mathcal{V}_0 = l_2\{\mathbb{Z}\} \tag{1}$$
$$\mathcal{V}_i = \operatorname*{Span}_k\{h_i(n - 2^i k)\} \tag{2}$$
$$\mathcal{Q}_i = \operatorname*{Span}_k\{f_i(n - 2^i k)\} \tag{3}$$
$$\mathcal{W}_i = \operatorname*{Span}_k\{g_i(n - 2^i k), g_i(1 - 2^i k - n)\} \tag{4}$$
$$l_2\{\mathbb{Z}\} = \mathcal{Q}_1 \oplus \mathcal{V}_1 \tag{5}$$
$$= \mathcal{W}_1 \oplus \mathcal{Q}_2 \oplus \mathcal{V}_2 \tag{6}$$
$$= \mathcal{W}_1 \oplus \mathcal{W}_2 \oplus \mathcal{Q}_3 \oplus \mathcal{V}_3 \tag{7}$$
$$= \mathcal{W}_1 \oplus \mathcal{W}_2 \oplus \mathcal{W}_3 \oplus \mathcal{Q}_4 \oplus \mathcal{V}_4. \tag{8}$$

Each line above corresponds to the decomposition by an l-scale filterbank, the last line being that of a four-scale filterbank. The nesting of approximation spaces generated by the four-scale filterbank is expressed as

$$\mathcal{V}_4 \subset (\mathcal{Q}_4 \oplus \mathcal{V}_4) \subset (\mathcal{W}_3 \oplus \mathcal{Q}_4 \oplus \mathcal{V}_4) \subset \cdots \subset l_2\{\mathbb{Z}\}.$$

E. Relationship with M-band Wavelet Bases

It should be noted that a relationship exists between the bases described in this paper and those described in [17]–[19], [29]. Those references describes a generalization of the two-band Daubechies wavelet basis to M-bands or, equivalently, an M-channel orthogonal filterbank with K zero moments for general M and K. In particular, for an M-band system, these references describe the shortest lowpass (scaling) filter with a specified number K of zero moments. We wish to note that for $K = 2$, this maximally regular filter (in the terminology of [29]) is identical to the lowpass filter $h_i(n)$ described above (with $i = M$).

As noted in [29], given the lowpass branch of an orthogonal filterbank, the remaining filters are not uniquely determined, in contrast with the two-band case. This makes the design of remaining channels more difficult, and although methods for obtaining a set of $M - 1$ filters to complete the filterbank are described in [29] (see also [31]), it can be difficult to control the characteristics of the resulting filters and, in particular, to regulate their lengths. For $K = 2$, the filters $f_i(n)$ and $g_i(n)$ described above give a way to complete the filterbank, given the maximally regular lowpass branch, in a way that reproduces the characteristics of a tree structured two-band system.

It should also be noted that the way in which the filters $f_i(n)$ and $g_i(n)$ complete the filterbank, given the maximally regular lowpass branch, differs from that suggested in [29]. In [29], a completion of the filterbank that approximates a uniform division of the frequency spectrum into M equal bands is suggested. Indeed, the motivation for the M-band system in [29] is not the improvement of time-localization properties while preserving the essential time–frequency tiling of the two-band DWT, but it is to provide a different tiling of the time–frequency plane that might better suite certain applications.

Certainly, given an M-band lowpass filter, we can complete the filterbank in a number of ways, one being the approximate uniform division of frequency and a second being a division in frequency similar to that provided by an iterated two-band system. In this paper, we have chosen the second and have used the greater generality to improve the time localization of the resulting basis.

F. Finite-Length Signals

The orthogonal discrete wavelet transform based on filterbank iteration is usually adapted to finite (power of 2) length data by periodizing the signal. Each output of the analysis filterbank is then periodic, and in this manner, an orthogonal transformation can be constructed for a finite interval. The same can be done for the slantlet filterbank, with results that are especially clean, due to the lengths of the the filters being powers of 2. Consider the orthogonal matrix of dimension 2^l representing the transform associated with an l-scale filterbank. In Fig. 5, a 16 × 16 example is illustrated for $l = 4$.

The first row of the matrix, which corresponds to $h_l(n)$, is simply a constant. The effect of periodizing the input results in an overlapping effect for $h_l(n)$

$$h_l(n) + h_l(n + 2^l) = b_{0,0} + b_{1,0} + (b_{0,1} + b_{1,1})n \tag{9}$$
$$= \frac{1}{\sqrt{m}} \tag{10}$$

for $n = 0, \ldots, 2^l - 1$, $m = 2^l$. The second row, corresponding to $f_l(n)$, is a linear function, as is shown in Fig. 5. Periodization results in an overlapping effect for $f_l(n)$, as it does for $h_l(n)$

$$f_l(n) + f_l(n + 2^l) = c_{0,0} + c_{1,0} + (c_{0,1} + c_{1,1})n \tag{11}$$
$$= \sqrt{\frac{3(m-1)}{m(m+1)}} - 2\sqrt{\frac{m}{m(m^2-1)}}n \tag{12}$$

for $n = 0, \ldots, 2^l - 1$, $m = 2^l$. Each of the remaining rows of the matrix consists of the sequences $g_i(n)$, its time reverse, and their shifts by 2^{i+1}, for $i = 1, \ldots, (l-1)$. Except for the first two rows, there is no overlapping effect at the boundaries of the matrix, as the supports are powers of two.

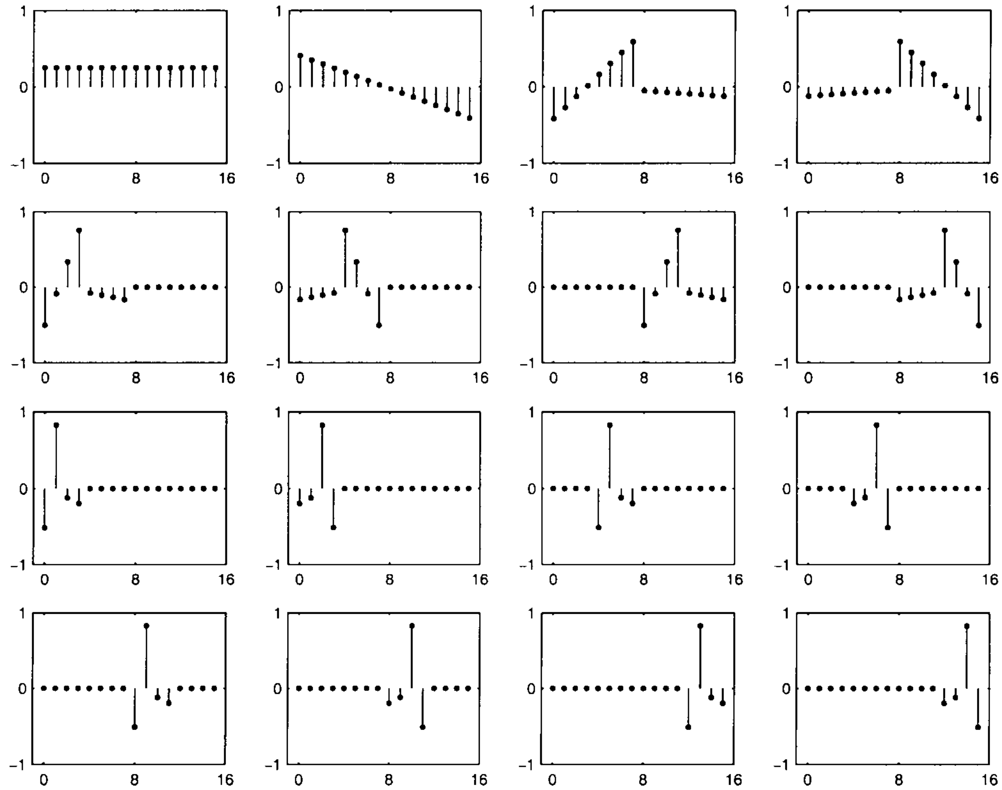

Fig. 5. Slantlet $(N = 16)$ basis. Vectors of the 16 × 16 orthogonal matrix associated with the four-scale slantlet filterbank.

G. Comparison with Slant Transform

Interestingly, the Haar basis can be obtained by downsampling the Walsh basis. Both are piecewise constant, but the Walsh transform serves as a minimal complexity DCT for frequency analysis, whereas the Haar transform, having basis functions of progressively shorter widths, gives a multiresolution decomposition. A piecewise linear basis that follows the spirit of the Walsh transform (in performing frequency analysis) is the *slant* transform [1], [7], [15], [23], [25], [26], [33], which has been used in Intel's "Indeo" video compression algorithm [8]. In a loose sense, the transform described in this paper is to the slant transform what the Haar transform is to the Walsh transform. The analogy is only loose, however, and their similarities suggest the name *slantlet* transform for the transform described in this paper.

H. Efficient Implementation

A key to the efficient implementation of the usual DWT is its tree structure. The long filters used to analyze coarse scales are implemented by a sequence of convolutions and downsampling. In the slantlet filterbank, it appears initially that an efficient implementation is not available for the lack of tree structure. However, an efficient implementation is possible, as is shown here. The efficient algorithm given below resembles closely the iterative procedure used to implement an iterated filterbank tree; therefore, the computational complexity is of the same order, although the code complexity may increase.

Because the filters are piecewise linear, each filter can be represented as the sum of a DC and a linear term. Due to the simple form of the filters $g_i(n)$, only four terms are needed to compute $y_i(n)$. Writing the output sample of channel i as an inner product

$$y_i(n) = \sum_{k=0}^{2^{i+1}-1} x(2^{i+1}n+k)g_i(k) \tag{13}$$

$$= \sum_{k=0}^{2^i-1} x(2^{i+1}n+k)(a_{0,0}+a_{0,1}k) + \sum_{k=2^i}^{2^{i+1}-1} x(2^{i+1}n+k)(a_{1,0}+a_{1,1}(k-2^i)) \tag{14}$$

$$= a_{0,0}\sum_{k=0}^{2^i-1} x(2^{i+1}n+k) + a_{0,1}\sum_{k=0}^{2^i-1} kx(2^{i+1}n+k) + a_{1,0}\sum_{k=0}^{2^i-1} x(2^{i+1}n+(k+2^i)) + a_{1,1}\sum_{k=0}^{2^i-1} kx(2^{i+1}n+(k+2^i)) \tag{15}$$

$$= a_{0,0}\mu_0(2n;i) + a_{1,0}\mu_0(2n+1;i) + a_{0,1}\mu_1(2n;i) + a_{1,1}\mu_1(2n+1;i) \tag{16}$$

where

$$\mu_0(n;i) = \sum_{k=0}^{2^i-1} x(2^i n+k) \tag{17}$$

$$\mu_1(n;i) = \sum_{k=0}^{2^i-1} kx(2^i n+k) \tag{18}$$

are types of DC and linear moments at scale i of the input signal $x(n)$. The same expressions are valid for the projections of $x(n)$ onto the time-reversed versions of $g(n)$, but the constants $a_{0,0}$, $a_{0,1}$, $a_{1,0}$, and $a_{1,1}$ are to be modified.

Note that as in the Haar DWT, the moments can be computed efficiently by a simple recursive algorithm that starts with the fine scale $i = 1$. The DC and linear moments at scale i can be computed from the DC and linear moments at the next finer scale $(i-1)$ by

$$\mu_0(n;i) = \mu_0(2n;i-1) + \mu_0(2n-1;i-1) \tag{19}$$

$$\mu_1(n;i) = \mu_1(2n;i-1) + \mu_1(2n-1;i-1) + 2^{i-1}\mu_0(2n-1;i-1). \tag{20}$$

The inverse can also be computed efficiently by making use of the values $\mu_0(n;i)$ and $\mu_1(n;i)$. For the efficient computation of the inverse, we first compute $\mu_0(n;l)$ and $\mu_1(n;l)$ from the DC and linear slantlet coefficients; we then compute $\mu_0(n;i)$ and $\mu_1(n;i)$ for decreasing values of i by updating μ_0 and μ_1 using the slantlet coefficients. Finally, with $i = 1$, the original signal $x(n)$ is obtained from μ_0 and μ_1 via the relation

$$x(2n) = \mu_0(n;1) \tag{21}$$

$$x(2n+1) = \mu_0(n;1) + \mu_1(n;1). \tag{22}$$

Therefore, even though the design of the filterbank is not based on an iterated filterbank, the computation of its output can be made efficient by a recursive method.

I. Shift Variance and Redundant Transform

It should be noted that slantlet filterbanks are more time varying than those based on filterbank iteration. Consider the highpass branch of the tree-structured filterbank in Figs. 1 and 3. The highpass channel is periodically time varying due to the downsampling, with a period of 2. On the other hand, the highpass channels of the slantlet filterbank are periodically time varying with period 4.

It is seen that the improvement with regard to time localization costs us not only the simple tree structure but also costs one greater shift variance. In some applications, that is a disadvantage. However, in denoising, the loss of shift variance can be overcome by turning to a redundant transform. With such a transform, shift invariance is retrieved by effectively including all shifts of the data and comes at the expense of a redundant representation. Interestingly, it has been shown that denoising via wavelet thresholding can yield superior results when carried out with this shift-invariant redundant (or stationary) wavelet transform [10], [20]. If memory and run-time requirements permit, the use of a redundant transform for denoising can be advantageous. In this case, redundant denoising is an application where the greater shift variance of the slantlet filterbank is not expected to be a significant drawback. A redundant shift-invariant version of the slantlet transform, in the sense of [10], is straightforward to derive and can be implemented in a similar way.

J. Denoising Example

In this denoising example, the behavior of the slantlet basis is compared with other wavelet bases having two vanishing moments: the D_2 basis, the biorthogonal-2,2 and -2,4 bases (see [13, p. 273]), and the piecewise linear semi-orthogonal (spline) bases (see [32, p. 147]). For the nonorthogonal bases, the DWT was carried out with symmetric extensions. A hard threshold was applied uniformly to each scale. We chose the signal to be the "Houston skyline" function by Guo because it is piecewise linear and has numerous discontinuities. Fig. 6 illustrates the results. Denoising with the slantlet transform yields the same artifacts and noise spikes, but for this example, they were generally reduced. Varying the threshold used and averaging over 200 realizations for each threshold, the curve illustrating the root-mean-square error in Fig. 6 was obtained. That figure shows that for this example, the slantlet transform gives an improvement. It indicates that on average, for thresholds between 0.12 and 0.24, the error with the slantlet is smaller than that obtained with D_2 for any threshold. That a wider choice of thresholds gives such results is important because in practice, of course, the best threshold for a particular example is unknown. It is interesting to note that for thresholds above 0.24, the semi-orthogonal (spline) bases perform better than do the biorthogonal bases in this example. Certainly, the most appropriate basis depends on the data and the noise level.

It should be noted that there are a variety of denoising techniques that go beyond simple thresholding that can produce dramatically improved results. For example, we have the shift-invariant transform of [10] and [20] mentioned above and the hidden-Markov model-based approach of [12].

K. Underlying Continuous-Time Wavelets

As noted in the Introduction, the slantlet basis is a special case of the multiwavelet bases described by Alpert [4]–[6], comprised of r scaling functions and r wavelet functions with r vanishing moments. The continuous-time multiwavelet basis of [6] with $r = 2$ is piecewise linear and discontinuous.[2] However, it is important to note that for these bases, the relationship between continuous-time and discrete-time versions is not as simple as it is for scalar wavelet bases (wavelet bases based on a single scaling function). In the scalar case, the discrete-time basis is obtained by iterated filtering and upsampling. However, the filterbank associated with Alpert's continuous-time multiwavelet bases with $r = 2$ does not yield the discrete-time slantlet basis due to important differences between scalar- and multiwavelet bases, as highlighted in [28]; in the terminology of [21] and [22], the multiwavelet basis is not *balanced*. To obtain a discrete-time version of the basis, Alpert used a Gram–Schmidt orthogonalization and considers the general case of r vanishing moments, whereas we use Gröbner bases to derive explicit solutions for the special case of 2 vanishing moments. The explicit solutions for the filters at

[2] Alpert's basis has $\psi_0(t)$ symmetric: $\psi_0(t) = \psi_0(t-T)$, and $\psi_1(t)$ anti-symmetric: $\psi_1(t) = -\psi_1(t-T)$. It is immediate that pairwise symmetry can be obtained by taking their sum and difference.

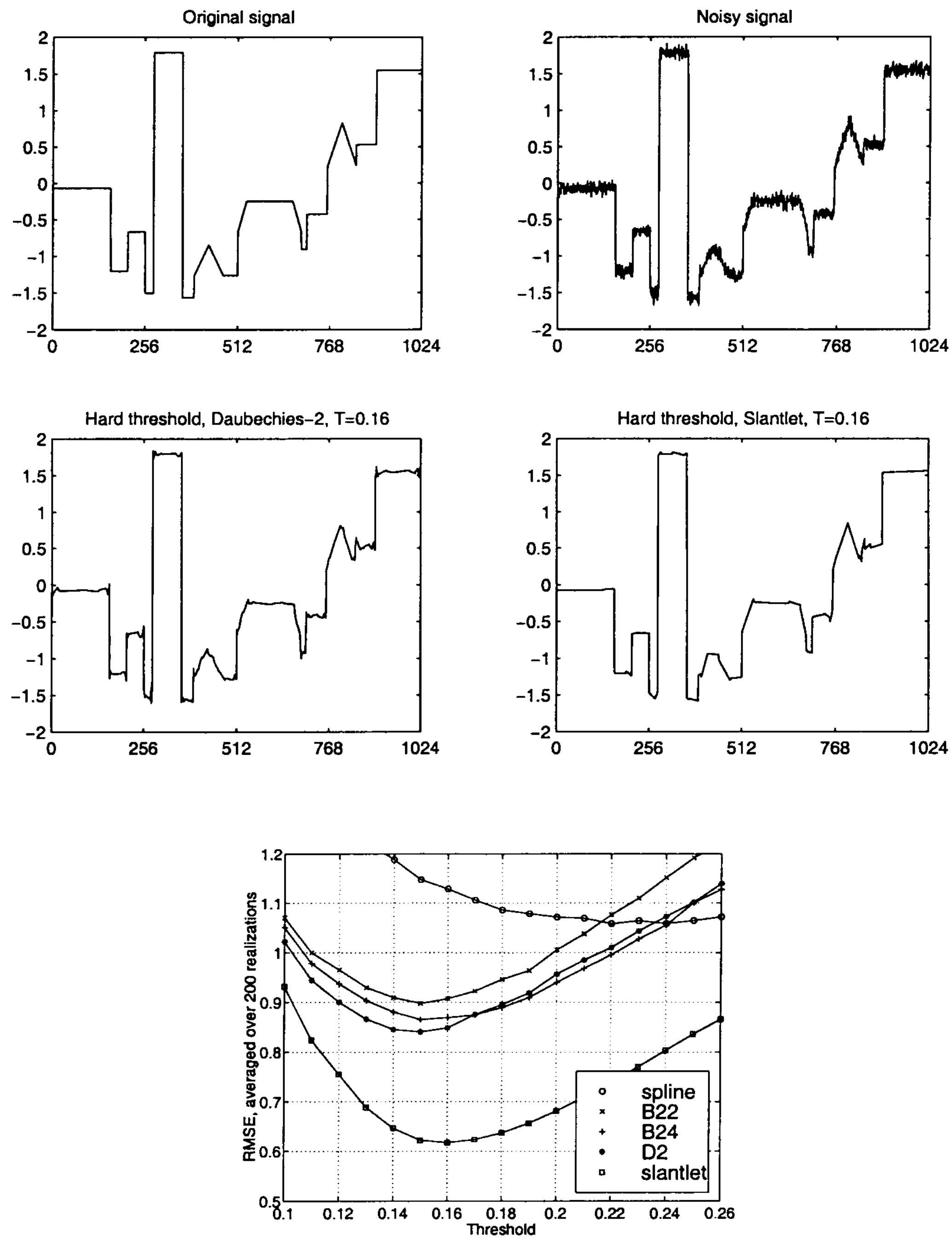

Fig. 6. Denoising via hard thresholding with the iterated D_2 filterbank and the slantlet DWT.

each scale are useful because they are required for the efficient implementation of the transform described in Section II-H.

The approach taken by Alpert addresses the extension of these bases to a higher number of vanishing moments; however, higher order extensions entail a higher number of separate functions/filters to analyze a signal at a single stage. The number of filters increases according to the order. For bases that are piecewise polynomial with degree $r - 1$, r vanishing moments requires r wavelet functions/filters.

L. Multidimensional Filterbanks

The generalization to the multidimensional case is not as straightforward as it is for iterated filterbank trees. Nevertheless, a 2-D filterbank can be obtained in a similar manner that is composed of separable filters, although the filterbank itself is not separable. In the 2-D case, the area of support of the filters approaches $(2/3)^2 = 4/9$ that of the iterated 2-D D_2 system. That is a reduction of the area of support by over one half, suggesting that in more than one dimension, the tradeoff between zero moments and time- localization becomes more significant. However, the smoothness properties of the 2-D slantlet and the separable 2-D D_2 transforms are different as well. While the highpass and bandpass filters of the 2-D slantlet filterbank annihilate linear polynomials in two variables, $an_1 + bn_2 + c$; the separable 2-D D_2 filterbank annihilates polynomials of the form $an_1n_2 + bn_1 + cn_2 + d$.

TABLE I
COMPARING THE ITERATED D_2 AND SLANTLET FILTERBANKS

	Iterated D_2	Slantlet
Orthogonal	y	y
Octave-band	y	y
Approximation order	2	2
Efficient implementation	y	y
Piecewise linear	n	y
Support at scale i	$3 \cdot 2^i - 2$	2^{i+1}

It should be emphasized that the slantlet transform is most appropriate for data that is piecewise linear and cannot be expected to be useful in the compression of natural images, for example. A description of the details of the 2-D slantlet transform will be available from the author.

III. CONCLUSION

The smoothing of data while preserving edges relatively well is an essential advantage of wavelets in denoising, and it depends in part on both the short support of the basis functions with respect to their scale and their number of vanishing moments. In addition, in the application of wavelet bases to image compression, the time localization and the number of zero moments of the basis are both important. Good time-localization properties lead to good representation of edges. Approximation order is important for sparse representation (compression) of smooth regions. However, short support and zero moments are competing criteria in the construction of wavelet filterbanks.

In this light, this paper presents an orthogonal filterbank for the discrete wavelet transform with two zero moments, where the filters are of shorter support than those of the iterated D_2 filterbank tree. Although not based on an iterated filterbank tree, the filterbank described in this paper retains the main desirable characteristics of the usual DWT filterbank, namely, orthogonality, an octave-band characteristic, a scale-dilation factor of 2, and an efficient implementation. Table I summarizes a comparison. A transform for finite length signals based on this filterbank is particularly clean due to the filter lengths being exact powers of two. The basis appears particularly well suited for piecewise linear signals, as does the Haar basis for piecewise constant signals. Improvement in a denoising example was also shown.

Matlab programs for the slantlet transform, its inverse, a shift-invariant (redundant) variant, and a 2-D version are available from the author or via the Internet at http://taco.poly.edu/selesi/.

ACKNOWLEDGMENT

The author wishes to thank H. W. Schüßler and P. Steffen of the Lehrstuhl für Nachrichtentechnik, Universität Erlangen-Nürnberg, H. Guo for providing his "Houston Skyline" function, and the anonymous reviewers.

REFERENCES

[1] N. Ahmed and K. R. Rao, *Orthogonal Transforms for Digital Signal Processing*. New York: Springer-Verlag, 1975.
[2] A. Aldroubi, M. Eden, and M. Unser, "Discrete spline filters for multiresolution and wavelets of l_2," *SIAM J. Math. Anal.*, vol. 25, no. 5, pp. 1412–1432, Sept. 1994.
[3] A. Aldroubi and M. Unser, "Oblique projections in discrete signal subspaces of l_2 and the wavelet transform," in *Proc. SPIE-Math. Imag.: Wavelet Appl. Signal Image Process.*, San Diego, CA, July 27–29, 1994, vol. 2303, pp. 36–46.
[4] B. Alpert, G. Beylkin, R. Coifman, and V. Rokhlin, "Wavelet-like bases for the fast solution of second-kind integral equations," *SIAM J. Sci. Comput.*, vol. 14, no. 1, pp. 159–184, Jan. 1993.
[5] B. K. Alpert, "Wavelets and other bases for fast numerical linear algebra," in *Wavelets: A Tutorial in Theory and Applications*, C. K. Chui, Ed. New York: Academic, 1992.
[6] ——, "A class of bases in l^2 for the sparse representation of integral operators," *SIAM J. Math. Anal.*, vol. 24, no. 1, pp. 246–262, Jan. 1993.
[7] M. M. Anguh and R. R. Martin, "A truncation method for computing slant transforms with applications to image coding," *IEEE Trans. Commun.*, vol. 43, pp. 2103–2110, June 1995.
[8] P. Bahl, P. S. Gauthier, and R. A. Ulichney, "PCWG's INDEO-C video compression algorithm," available WWW: http://www.europe.digital.com/info/DTJK04/, Apr. 11, 1996.
[9] C. S. Burrus, R. A. Gopinath, and H. Guo, *Introduction to Wavelets and Wavelet Transforms*. Englewood Cliffs, NJ: Prentice-Hall, 1997.
[10] R. R. Coifman and D. L. Donoho, "Translation-invariant de-noising," in *Wavelets and Statistics, Lecture Notes*, A. Antoniadis, Ed. New York: Springer-Verlag, 1995.
[11] R. M. Corless, *Essential Maple: An Introduction for Scientific Programmers*. New York: Springer-Verlag, 1995.
[12] M. S. Crouse, R. D. Nowak, and R. G. Baraniuk, "Wavelet-based signal processing using hidden markov models," *IEEE Trans. Signal Processing*, vol. 46, pp. 886–902, Apr. 1998.
[13] I. Daubechies," *Ten Lectures on Wavelets*. Philadelphia, PA: SIAM, 1992.
[14] D. L. Donoho, "De-noising by soft-thresholding," *IEEE Trans. Inform. Theory*, vol. 41, pp. 613–627, May 1995.
[15] H. Enomoto and K. Shibata, "Orthogonal transform coding system for television signals," in *Proc. 1971 Symp. Appl. Walsh Functions*, 1971, pp. 11–17.
[16] G.-M. Greuel, G. Pfister, and H. Schönemann, "Singular reference manual," in *Reports on Computer Algebra*, Cent. Comput. Algebra, Univ. Kaiserslautern, no. 12, May 1997. Available [Online] http://www.mathematik.uni-kl.de/∼zca/Singular.
[17] P. N. Heller, "Rank M wavelets with N vanishing moments," *SIAM J. Math. Anal.*, vol. 16, no. 2, pp. 502–519, 1995.
[18] J. Kautsky, "An algebraic construction of discrete wavelet transforms," *Appl. Math.*, vol. 3, no. 38, pp. 169–193, 1993.
[19] J. Kautsky and R. Turcajova, "Pollen product factorization and construction of higher multiplicity wavelets," *Linear Algebra Appl.*, vol. 222, p. 241, 1995.
[20] M. Lang, H. Guo, J. E. Odegard, C. S. Burrus, and R. O. Wells, Jr., "Noise reduction using an undecimated discrete wavelet transform," *IEEE Signal Processing Lett.*, vol. 3, pp. 10–12, Jan. 1996.
[21] J. Lebrun and M. Vetterli, "Balanced multiwavelets theory and design," *IEEE Trans. Signal Processing*, vol. 46, pp. 1119–1124, Apr. 1998.
[22] J. Lebrun and M. Vetterli, "High order balanced multiwavelets," in *Proc. IEEE Int. Conf. Acoust., Speech, Signal Process. (ICASSP)*, Seattle, WA, May 12–15, 1998.
[23] P. C. Mali, B. B. Chaudhuri, and D. D. Majumder, "Some properties and fast algorithms of slant transform in image processing," *Signal Process.*, vol. 9, pp. 233–244, Dec. 1985.
[24] T. Ogden and E. Parzen, "Data dependent wavelet thresholding in nonparametric regression with change-point applications," *Comput. Stat. Data Anal.*, vol. 22, pp. 53–70, 1996.
[25] W. K. Pratt, L. R. Welch, and W. H. Chen, "Slant transforms for image coding," in *Proc. 1972 Symp. Appl. Walsh Functions*, 1972, vol. AD-744650, pp. 229–234.
[26] W. K. Pratt, L. R. Welch, and W. H. Chen, "Slant transform image coding," *IEEE Trans. Commun.*, vol. COMM-22, pp. 1075–1093, Aug. 1974.
[27] J. E. Richwine, "Bayesian estimation of change-points using Haar wavelets," M.S. Thesis, Univ. South Carolina, Columbia, 1996.
[28] I. W. Selesnick, "Multiwavelet bases with extra approximation properties," *IEEE Trans. Signal Processing*, vol. 46, pp. 2998–2909, Nov. 1998.

[29] P. Steffen, P. Heller, R. A. Gopinath, and C. S. Burrus, "Theory of regular M-band wavelet bases," *IEEE Trans. Signal Processing*, vol. 41, pp. 3497–3511, Dec. 1993.

[30] G. Strang and T. Nguyen, *Wavelets and Filterbanks*.Wellesley, MA: Wellesley-Cambridge, 1996.

[31] J. Tian and R. O. Wells, Jr., "A fast implementation of wavelet transform for m-band filterbanks," in *Proc. SPIE 3391 Wavelet Applications V*, H. H. Szu, Ed., 1998.

[32] M. Unser, A. Aldroubi, and M. Eden, "A family of polynomial spline wavelet transforms," *Signal Process.*, vol. 30, no. 2, pp. 141–162, Jan. 1993.

[33] J.-F. Yang and Ch.-P. Fan, "Centralized fast slant transform algorithms," *IEICE Trans. Fundamentals Electron., Commun., Comput. Sci.*, vol. E80-A, no. 4, pp. 705–711, Apr. 1997.

Ivan W. Selesnick (M'98) received the B.S., M.E.E., and Ph.D. degrees in electrical engineering in 1990, 1991, and 1996, respectively, from Rice University, Houston, TX.

He received a DARPA-NDSEG fellowship in 1991. He has been employed by McDonnell Douglas and IBM, working on neural networks and expert systems. He spent part of 1997 at the the Lehrstuhl für Nachrichtentechnik Universität Erlangen-Nürnberg, Erlangen, Germany. He is currently an Assistant Professor in the Electrical Engineering Department, Polytechnic University, Brooklyn, NY. His current research interests are in the area of digital signal processing, in particular, fast algorithms for digital signal processing, digital filter design, the theory and application of wavelets, and the application of Gröbner bases.

Dr. Selesnick's Ph.D. dissertation received the Budd Award for Best Engineering Thesis at Rice University in 1996 and an award from the Rice-TMC chapter of Sigma Xi. In 1997, he received an Alexander von Humboldt Award. He is a member of Eta Kappa Nu, Phi Beta Kappa, Tau Beta Phi, and Sigma Xi.